J Electroceram (2006) 16:571–574
DOI 10.1007/s10832-006-9921-1

Structural properties and dopant-modified bandgap energies of $Ba_{0.5}Sr_{0.5}TiO_3$ thin films grown on $LaAlO_3$ substrates

Y. B. Zheng · S. J. Wang · L. B. Kong · S. Tripathy · A. C. H. Huan · C. K. Ong

© Springer Science + Business Media, LLC 2006

Abstract $Ba_{0.5}Sr_{0.5}TiO_3$ thin films doped with different concentration of Ti, Mg and Al dopants were prepared by pulsed laser deposition technique on $LaAlO_3$ substrates. The crystalline properties of these doped thin films were studied using X-ray diffraction, micro-Raman scattering, atomic force microscopy, and transmission electron microscopy. The bandgap energies of BST thin films are determined from the transmission and absorption measurements by the ultraviolet-visible spectrophotometer. It was found out that the bandgap energies of the doped BST thin films depend strongly on the dopant concentration.

Keywords Band structure · Dopants · Ferroelectric thin films

1 Introduction

$Ba_xSr_{1-x}TiO_3$ $(0 \leq x \leq 1)$ is one of the well-studied perovskite material systems suitable for applications in high-density dynamic random access memories (DRAMs), millimeter microwave integrated circuits (MMICs) and electro-optic devices [1–6]. For high performance devices, such as voltage tunable filter and phase shifter, it is necessary to decrease the dielectric loss of $Ba_xSr_{1-x}TiO_3$ in the form of thin film. The small bandgap energy around 3.5 eV cannot meet the requirement of high barrier height and low leakage current density for DRAM applications. Recently, $Ba_xSr_{1-x}TiO_3$ thin films doped with additional elements or oxides, including Al_2O_3, TiO_2, MgO, W and Mn, demonstrated the improvement of dielectric and electrical properties [7–14]. The enhancement of bandgap energies has also been found in Al-doped $Ba_{0.5}Sr_{0.5}TiO_3$ (BST) thin films [15]. In the present study, we systematically investigated the bandgap energies and structural properties of Ti-, Mg- and Al-doped BST thin films using the combination of various characterization techniques.

2 Experimental procedures

The Ti-, Mg- and Al-doped BST thin films were grown on (100) $LaAlO_3$ single crystal substrates by pulsed laser deposition (PLD) with a KrF excimer laser, operating at repetition rate of 5 Hz with an average pulse energy of 250 mJ. The targets of TiO_2, MgO or Al_2O_3 plate were attached on the surface of sintered BST, respectively. The coverage area of TiO_2/MgO/Al_2O_3 plate over BSTdetermined the concentration of Ti/Mg/Al in the deposited thin films. The deposition was carried outat a substrate temperature of 650°C and post-deposition annealing wasdone in the PLD chamber at the same temperature butwith a higher oxygen pressure. In total, ten samples were prepared, including one pure BST thin films, three each of Ti-, Mg, and Al-doped BST thin films. The pure BST thin film was abbreviated to BST0 and the Ti-, Mg- and Al-doped BST thin films were sequentially

Y. B. Zheng (✉) · S. J. Wang · S. Tripathy · A. C. H. Huan
Institute of Materials Research & Engineering, 3 Research Link, Singapore 117602

S. J. Wang
e-mail: sj-wang@imre.a-star.edu.sg

L. B. Kong
Temasek Laboratory, National University of Singapore, Singapore, 119260

A. C. H. Huan
Division of Physics and Applied Physics, Nanyang Technological University, Singapore 637616

C. K. Ong
Department of Physics, National University of Singapore, Singapore 117542

Table 1 The Ti, Mg and Al concentration (at %) in the BST samples

Conc. / Type	Number			
	0	1(%)	2(%)	3(%)
BSTT	0	2	10	19
BSTM	0	2	11	17
BSTA	0	2	9	14

abbreviated to BSTT1, BSTT2, BSTT3, BSTM1, BSTM2, BSTM3, BSTA1, BSTA2 and BSTA3. The dopant concentration in the films was characterized by using X-ray photoelectron spectroscopy (XPS) and analyzed by using peak fitting, as listed in Table 1. The thickness of grown thin films was around 500 nm measured by scanning electron microscopy (SEM). The grain size estimated from atomic force microscopy (AFM) and transmission electron microscopy (TEM) is around 15 nm in diameter.

The optical transmission spectra were recorded in the wavelength range of 200–900 nm using double beam UV-VIS spectrophotometer (UVS). A Philips CM 300 TEM and a Digital Multimode Nanoscope IIIA AFM were used to characterize the microstructures. X-ray diffraction (XRD) scans were recorded using a GADDS XRD system. The micro-Raman measurements were carried out at room temperature using the JY-T64000 triple monochromator system attached to a liquid nitrogen cooled CCD detector.

3 Results and discussion

In the optical absorption-related experiments, it is well known that the fundamental absorption refers to the valence band (VB)-to-conduction band (CB) transition, from which the bandgap energy (E_g) can be estimated by assuming a direct transition between the bands [16]. The absorption coefficient α as a function of photo energy $h\nu$ can be expressed as

$$(\alpha h\nu)^2 = C(h\nu - E_g) \quad (1)$$

where α is the absorption coefficient, h is Plank's constant, and ν is the light frequency and C is a constant. Therefore, the bandgap energies of the thin films can be obtained by extrapolating the linear portion of the curves relating $(\alpha h\nu)^2$ and $h\nu$ to $(\alpha h\nu)^2 = 0$. Here, we have measured the optical transmission spectra of the BST thin films using UV-visible spectrophotometer, from which the evolution of $(\alpha h\nu)^2$ as a function of $h\nu$ was derived and thus the bandgap energies of the films were obtained. Figure 1 shows the bandgap energies versus the dopant concentration and the inset illustrates the typical curve of $(\alpha h\nu)^2$ as a function of photo energy for the BST thin films and the way to accurately obtain the bandgap energy value (denoted by arrow). We can see that the bandgap energies in all the cases increased with an increase in dopant concentration.

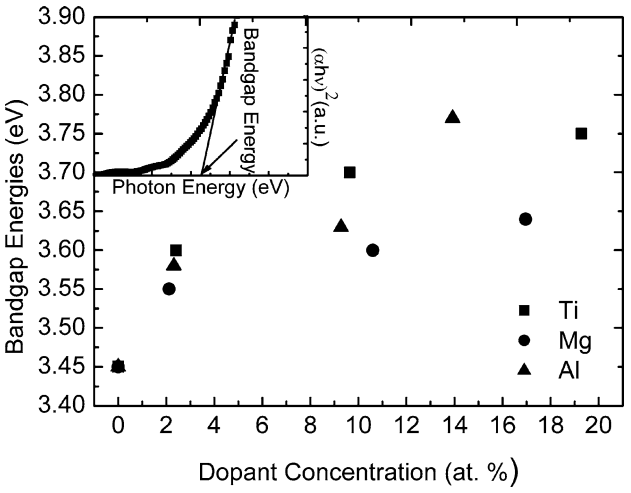

Fig. 1 The bandgap energies versus the dopant concentration of BST thin films. The inset illustrates the typical curve of $(\alpha h\nu)^2$ as a function of $h\nu$ and the way to accurately obtain the bandgap energy value (denoted by an arrow)

To clarify the origin of the increased bandgap energies due to an increased dopant concentration, the effects of various dopants on the structural properties of the BST thin films have been investigated. Figure 2 shows the XRD spectra of the pure and doped BST films. Figure 2(a) represents XRD spectra of the pure and Ti-doped BST thin films, from which we can see that BST (100) and (200) peaks became broader and weaker as the Ti concentration increases. This implies that the Ti-doped BST films possess smaller grains and presence of an amorphous phase could broaden the peaks [10]. BST (110) and TiO_2 peak appeared in BSTT3 and this indicates the polycrystalline structure and the existence of TiO_2 phase in BST with highest Ti-doping [17]. Figures 2(b) and (c) are the spectra of Mg- and Al-doped BST thin films, respectively. Similar to the case of Ti-doped BST, the broadening and weakening of BST (100) and (200) peaks upon increasing Mg and Al concentration indicates smaller grain size and existence of an amorphous phase in the samples. Polycrystalline structure and MgO phase appeared in BSTM3 whereas a new unidentified phase appeared in BSTA3. The existence of polycrystalline structures with smaller grains and amorphous phase in the doped BST thin films were further confirmed by AFM and TEM (not shown). Similar observations are also reported by other researchers [13, 14].

From XRD observations, we have also seen that both Ti and Mg doping in BST results in a shift of (200) peak to lower 2θ values, which indicates an increase in the c-lattice constant. Such a peak shift in the XRD spectra in doped BST

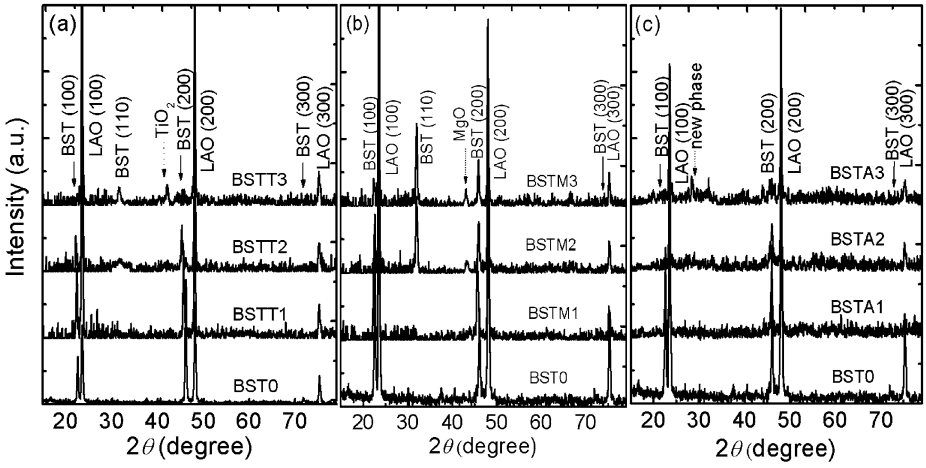

Fig. 2 XRD spectra of the samples: (a) pure and Ti-doped BST thin films; (b) pure and Mg-doped BST thin films; (c) pure and Al-doped BST thin films

films implies the existence of an in-plane compressive stress component. In order to characterize the stress states in the dopant modified BST films, we have carried out a systematic micro-Raman spectroscopic study. It is well known that lattice dynamics of perovskites films determine the fundamentals of phase transitions. Raman spectroscopy measurements on doped BST thin films would provide additional information such as the contribution of biaxial stress and its effect on the electronic bandgap. In general, the confinement of phonons in the films with small grains leads to broadening and phonon softening and the phonon wave numbers are also expected to shift towards higher/lower values depending upon the compressive/tensile nature of the stress in the films [4, 18, 19]. To obtain notable trends in the stress of the doped BST thin films, one of the stress sensitive hard modes, TO_4: A_1(TO), has been studied in detail [20]. Figure 3 shows the Raman spectra of the thin films after background signal was deducted. Figure 3(a) is the spectra of the pure and Ti-doped BST thin films, from which we can see that the peak of TO_4 mode broadened and shifted towards higher values when Ti concentration was increased. A large shift of 31 cm^{-1} was obtained for BSTT3 sample. We believe that such a large shift is a combined effect of the total stress and the smaller grains in the doped BST thin films. Thus, it was found out that Ti doping has caused an increase in the compressive strain component in these BST films.

In contrast, the TO_4 mode in the Raman spectra of Mg- and Al-doped BST thin films showed no significant blue shift besides broadening, as shown in Figs. 3(b) and (c), respectively. This indicates that doping Mg and Al caused the compressive stress relaxation in the BST thin films. Such peak shift is usually compensated by the grain size effect.

From the theoretical calculation based on density functional theory, it was found out that the bandgap of BST is dominated by the Ti atoms in perfect crystal. There is no significant increase in the direct bandgap energies between pure and Mg-doped BST films. The details of such calculations will be published elsewhere. Therefore, an increase in the bandgap energy of semiconductor thin films could be assigned to the quantum-size effect when the crystallite size became very small [21, 22]. The existence of amorphous phase and polycrystalline domains will modify the bandgap

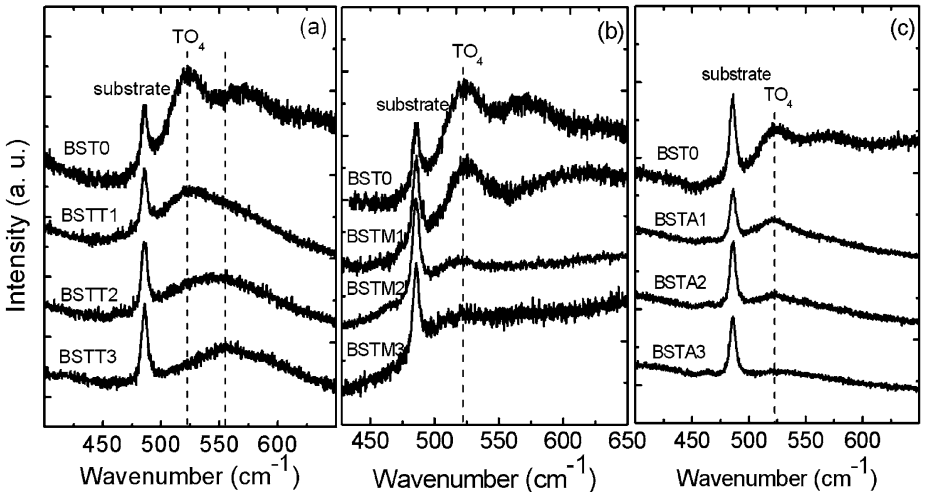

Fig. 3 Raman spectra of TO_4: A_1(TO) mode of the samples: (a) pure and Ti-doped BST thin films; (b) pure and Mg-doped BSTthin films; (c) pure and Al-doped BSTthin films

energy of the film [23]. The modification of bandgap energy by stress in the thin films has been reported [24, 25]. And for some cases it was also believed that polycrystalline thin films had higher bandgap energies than single crystals [26]. Therefore, we believe that the increase of bandgap energies of Ti-, Mg- and Al-doped BST thin films could be due to a combination of quantum-size effect in small grains, existence of amorphous phase, as well as biaxial stress in the films as confirmed by XRD, AFM, TEM and micro-Raman measurements.

4 Conclusions

In conclusion, the bandgap energies of Ti-, Mg- and Al-doped BST thin films prepared by PLD have been studied and the structural properties are investigated using various characterization techniques. Increase in dopant concentration leads to a smaller grain size and induce the formation of amorphous phase in the films. Both Mg and Al caused compressive stress relaxation in the films, while Ti dopant caused an increased compressive stress. The increase of the bandgap energies of the doped films is believed to be associated with a combined effect of quantum-size effect, existence of amorphous phase, and presence of biaxial stress in the BST films. At higher dopant concentration, the effect of polycrystalline domains could further significantly contribute to the optical and dielectric properties.

References

1. S.Y. Hou, J. Kwo, R.K. Watts, and J.Y. Cheng, *Appl. Phys. Lett*., **67**, 1387 (1995).
2. C.L. Chen, J. Shen, S.Y. Chen, G.P. Luo, C.W. Chu, F.A. Miranda, F.W. Wan Keuls, J.C. Jiang, E.I. Meletis, and H.Y. Chang, *Appl. Phys. Lett*., **78**, 652 (2001).
3. J.S. Lee, H. Wang, S.Y. Lee, S.R. Foltyn, and Q.X. Jia, *Appl. Phys. Lett.,* **83**, 5494 (2003).
4. F.M. Pontes, E.R. Leite, D.S.L. Pontes, E. Longo, E.M.S. Santos, S. Mergulhao, P.S. Pizani, F. Lanciotti, Jr., T.M. Boschi, and J.A. Varela, *J. Appl. Phys*., **91**, 5972 (2002).
5. Y.P. Wang and T.Y. Tseng, *J. Mater. Sci*., **34**, 4573 (1999).
6. B. Panda, A. Dhar, G.D. Nigam, D. Bhattacharya, and S.K. Ray, *Thin Solid Films,* **332**, 46 (1998).
7. I. Takeuchi, H. Chang, C. Gao, P.G. Schultz, X.D. Xiang, R.P. Sharma, M.J. Downes, and T. Venkatesan, *Appl. Phys. Lett*., **73**, 894 (1998).
8. H.D. Wu and F.S. Barnes, *Integr. Ferroelectr*., **22**, 811 (1998).
9. H. Chang, I. Takeuchi, and X.D. Xiang, *Appl. Phys. Lett.,* **74**, 1165 (1999).
10. Q.X. Jia, B.H. Park, B.J. Gibbons, J.Y. Huang, and P. Lu, *Appl. Phys. Lett*., **81**, 114 (2002).
11. E. Ngo, P.C. Joshi, M.W. Cole, and C.W. Hubbard, *Appl. Phys. Lett*. **79**, 248 (2001).
12. K.B. Chong, L.B. Kong, L.F. Chen, L. Yan, C.Y. Tan, T. Yang, C.K. Ong, and T. Osipowicz, *J. Appl. Phys.,* **95**, 1416 (2004).
13. M.W. Cole, W.D. Nothwang, C. Hubbard, E. Ngo, and M. Ervin, *J. Appl. Phys*., **93**, 9218 (2003).
14. M.W. Cole, C. Hubbard, E. Ngo, M. Ervin, M. Wood, and R.G. Geyer, *J. Appl. Phys*., **92**, 475 (2002).
15. Y.B. Zheng, S.J. Wang, A.C.H. Huan, C.Y. Tan, L. Yan, and C.K. Ong, *Appl. Phys. Lett.*, **86**, 112910 (2005).
16. D.H. Bao, X. Yao, N. Wakiya, K. Shinozaki, and N. Mizutani, *Appl. Phys. Lett*., **79**, 3767 (2001).
17. J. Im, O. Auciello, P.K. Baumann, S.K. Streiffer, D.Y. Kaufman, and A.R. Krauss, *Appl. Phys. Lett.,* **76**, 625 (2000).
18. P.S. Dobal, A. Dixit, R.S. Katiyar, D. Garcia, R. Guo, and A.S. Bhalla, *J. Raman Spectrosc*., **32**, 147 (2001).
19. D. Barsani, P.P. Lottici, and X.Z. Ding, *Appl. Phys. Lett*., **72**, 73 (1998).
20. J.A. Sanjurjo, E. Lopez-Cruz, and G. Burns, *Phys. Rev. B*, **28**, 7260 (1983).
21. Y. Wang and N. Herron, *J. Phys. Chem*., **95**, 525 (1991).
22. G. Hodes, A.A. Yaron, F. Decker, and P. Motisuka, *Phys. Rev. B*, **36**, 4215 (1987).
23. F. Tcheliebou, H.S. Ryu, C.K. Hong, W.S. Park, and S. Baik, *Thin Solid Films*, **305**, 30 (1997).
24. C. Merzy, M. Kunzery, U. Kaufmanny, I. Akasakiz, and H. Amanoz, *Semicond. Sci. Technol*., **11**, 712 (1996).
25. W.L. Ng, M.A. Lourenco, R.M. Gwilliam, S. Ledain, G. Shao, and K.P. Homewood, *Nature,* **410**, 192 (2001).
26. D.H. Bao, H.S. Gu, and A.X. Kuang, *Thin Solid Films*, **312**, 37 (1998).